Title
Simultaneous fMRI–PET of the opioidergic pain system in human brain

Journal
NeuroImage, 102(0 2)

ISSN
1053-8119

Authors
Wey, Hsiao-Ying
Catana, Ciprian
Hooker, Jacob M
et al.

Publication Date
2014-11-01

DOI
10.1016/j.neuroimage.2014.07.058

Peer reviewed

NeuroImage xxx (2014) xxx–xxx

Contents lists available at ScienceDirect

NeuroImage

journal homepage: www.elsevier.com/locate/ynimg

Simultaneous fMRI–PET of the opioidergic pain system in human brain

Hsiao-Ying Wey [a,*], Ciprian Catana [a], Jacob M. Hooker [a], Darin D. Dougherty [a,b], Gitte M. Knudsen [c], Danny J.J. Wang [d], Daniel B. Chonde [a], Bruce R. Rosen [a], Randy L. Gollub [a,b], Jian Kong [a,b,**]

[a] Athinoula A Martinos Center for Biomedical Imaging, Department of Radiology, Massachusetts General Hospital, Harvard Medical School, Charlestown, MA 02129, USA
[b] Department of Psychiatry, Massachusetts General Hospital, Harvard Medical School, Charlestown, MA 02129, USA
[c] Neurobiology Research Unit, Center for Integrated Molecular Brain Imaging, Rigshospitalet and University of Copenhagen, Denmark
[d] Ahmanson-Lovelace Brain Mapping Center, Department of Neurology, University of California at Los Angeles, CA 90095, USA

ARTICLE INFO

Article history:
Accepted 28 July 2014
Available online xxxx

Keywords:
Simultaneous MRI/PET
Neurotransmission
Hemodynamic response
Opioid receptor
Pain

ABSTRACT

MRI and PET provide complementary information for studying brain function. While the potential use of simultaneous MRI/PET for clinical diagnostic and disease staging has been demonstrated recently; the biological relevance of concurrent functional MRI–PET brain imaging to dissect neurochemically distinct components of the blood oxygenation level dependent (BOLD) fMRI signal has not yet been shown. We obtained sixteen fMRI–PET data sets from eight healthy volunteers. Each subject participated in randomized order in a pain scan and a control (nonpainful pressure) scan on the same day. Dynamic PET data were acquired with an opioid radioligand, [^{11}C]diprenorphine, to detect endogenous opioid releases in response to pain. BOLD fMRI data were collected at the same time to capture hemodynamic responses. In this simultaneous human fMRI–PET imaging study, we show co-localized responses in thalamus and striatum related to pain processing, while modality specific brain networks were also found. Co-localized fMRI and PET signal changes in the thalamus were positively correlated suggesting that pain-induced changes in opioid neurotransmission contribute a significant component of the fMRI signal change in this region. Simultaneous fMRI–PET provides unique opportunities allowing us to relate specific neurochemical events to functional hemodynamic activation and to investigate the impacts of neurotransmission on neurovascular coupling of the human brain in vivo.

Introduction

The tremendous potential for advancing clinical and basic neuroscience enabled by the newest generation of hybrid magnetic resonance imaging (MRI) and positron emission tomography (PET) (Catana et al., 2006) has yet to be achieved. While its potential use for clinical diagnostic and disease staging has been demonstrated (Catana et al., 2012; Drzezga et al., 2012); the biological relevance of simultaneous functional MRI–PET neuroimaging to dissect neurochemically distinct components of the blood oxygenation level dependent (BOLD) signal has not yet been shown. FMRI reveals detailed spatial and temporal patterns of hemodynamic responses reflecting neuronal activation that is a composite of all neurochemical events (Falkenberg et al., 2012; Jenkins, 2012; Muthukumaraswamy et al., 2012; Northoff et al., 2007). PET can be used to provide a simultaneous signal of neuroreceptor binding, neurotransmitter synthesis, reuptake or release specific to a single neuroreceptor system. To date, insights into the contributions of specific neurotransmitter systems to time varying changes in the BOLD signal have been provided by studies in humans using magnetic resonance spectroscopy (MRS). MRS studies have shown that the amplitudes of induced fMRI responses are related to the basal glutamate levels in the dorsal anterior cingulate cortex (Falkenberg et al., 2012), and that resting GABA concentrations are positively correlated with the task-evoked negative fMRI responses in the perigenual cingulate cortex and in the visual cortex (Muthukumaraswamy et al., 2012; Northoff et al., 2007). However, MRS has limited spatial coverage and resolution, and it is challenging to measure neurotransmitters other than the major neurotransmitters such as glutamate and GABA. Pre-clinical pharmacological MRI studies using specific agonist or antagonist drugs of selective receptor systems are beginning to pick out neuroreceptor specific components of fMRI signals (Jenkins, 2012). However, the application of pharmacological MRI to humans is limited due to the pharmacological doses involved. Simultaneous fMRI–PET offers a valuable means to probe specific neurochemical contributions to the composite BOLD signal while preserving the improved spatial and temporal resolution.

Opioid receptors are widely distributed throughout the central and peripheral nervous systems where they are known to modulate

* Correspondence to: H.-Y. Wey, Athinoula A. Martinos Center for Biomedical Imaging, Department of Radiology, Massachusetts General Hospital, Harvard Medical School, 149 13th Street, Charlestown, MA 02129, USA.
** Correspondence to: J. Kong, Department of Psychiatry, Massachusetts General Hospital, Harvard Medical School, 149 13th Street, Charlestown, MA 02129, USA.
E-mail addresses: wey@nmr.mgh.harvard.edu (H.-Y. Wey), kongj@nmr.mgh.harvard.edu (J. Kong).

http://dx.doi.org/10.1016/j.neuroimage.2014.07.058
1053-8119/

pain sensation. BOLD activation in humans in response to noxious stimulation is widespread, yet regionally specific and consistent, commensurate with the subjective experience of pain that includes sensory, affective and cognitive aspects. To investigate where within this pain activated network of brain regions the opioid modulation occurs, we examined the regional endogenous opioid displacement from opioid receptors as measured by the nonselective opioid receptor radioligand [^{11}C]diprenorphine ([^{11}C]DPN), during the administration of pressure cuff pain as compared with non-painful pressure. A decrease in PET radioligand binding potential (BP_{ND}) is typically interpreted as reflecting increased regional endogenous opioid release or receptor internalization (Laruelle, 2000). Although early PET imaging studies have implemented [^{11}C]DPN to investigate opioid receptor alternations in neuropathic pain conditions (Maarrawi et al., 2007; Willoch et al., 1999), to the best of our knowledge, it has not been used to investigate dynamic radioligand displacements prolonging pressure pain. BOLD fMRI was acquired concurrently to investigate the temporal and spatial patterns of functional hemodynamic changes evoked by pain. In this study, using experimental pressure pain and an opioid radioligand as a model, we present simultaneously collected fMRI–PET data in humans to investigate 1) BOLD signal changes evoked by pressure pain and non-painful pressure; 2) the engagement of the opioid system during pressure pain; and most importantly, 3) how opioid binding potential changes relate to BOLD fMRI responses.

Materials and methods

Subjects

Eleven healthy volunteers participated in this study with each subject underwent two PET/MRI scans. Three subjects did not finish the study because of not tolerating long scan duration. We successfully obtained sixteen fMRI–PET data sets from eight healthy volunteers (4 males, 4 females; mean age ± SD.: 24.1 ± 2.7). Each subject participated in randomized order in a pain scan and a control (non-painful pressure) scan on the same day. The Institutional Review Board at the Massachusetts General Hospital approved the study. All subjects provided written informed consent in accordance with the Human Research Committee of the Massachusetts General Hospital.

Behavioral session

Each subject was screened with a brief physical examination and medical history evaluation. Subjects diagnosed with medical or psychiatric illness or who used psychotropic medications in the past were excluded.

Subjects who were cleared for participation were familiarized with the noxious stimuli and rating procedures. Series of pressure stimuli were delivered on the subject's left lower leg (calf muscle) using a Velcro-adjusted pressure cuff (SC12D; Hokanson Inc., Bellevue, WA, USA) connected to a rapid cuff inflator (Hokanson E20, Hokanson Inc., Bellevue, WA, USA). Position of the cuff was noted in order to replicate the cuff placement during imaging. Multiple series of stimuli were applied to confirm the stability of subject's subjective ratings as well as to determine proper stimulus intensity for each subject to be used subsequently in the imaging session. The pain calibration procedures began with an ascending sequence of 8 stimuli with a starting pressure of 90 mm Hg and a 30 mm Hg stepping interval. Each stimulus was given for 30 s, followed by a 30 s rest. During the rest period, subjects were asked to report a subjective pain intensity rating according to the Gracely Intensity Scale in which 0 indicates no pain and 20 indicates the most intense pain tolerable (Gracely et al., 1978). The ascending sequence was terminated earlier if a pain intensity rating of 17/20 was obtained prior to completion of the sequence. The ascending sequence was repeated, and the pain intensity ratings for each stimulus intensity from the two sequences were averaged to determine the pressure to be used for subsequent testing. The pressures corresponding to pain intensity ratings of 5 and 15 were chosen as Low and High pain respectively. According to the descriptors provided in the Gracely scale, intensity ratings of 5 and 15 correspond to "weak" and "strong" pain levels respectively. One to two random (a mix of four Low and four High pain pressures) and identical (eight High pain pressures) sequences were administered to confirm rating consistency. Similar methods have been used in several studies from our lab (Kong et al., 2006a, 2006b, 2008).

Radiotracer synthesis

[^{11}C]DPN was synthesized at the Martinos Center for Biomedical Imaging using a modified version of published methods (Luthra et al., 1994). Briefly, the desmethyl precursor (ABX) was dissolved in dimethylformamide (300 μL) and treated with sodium hydride (5 mg) then [^{11}C]methyl iodide at 95 °C for 2 min. Following HPLC purification, the diluted product fraction was concentrated using solid-phase extraction and formulated in ethanol (1 mL) and 0.9% saline (9 mL). Typical radiochemical yield was 15–20%, decay-corrected with respect to initial [^{11}C]methyl iodide trapped in the reactor. The amount of diprenorphine injected was 3.35 ± 0.90 μg, activity: 10.77 ± 1.4 mCi, specific activity: 2.04 ± 0.40 mCi/mmol. The use of this radiopharmaceutical was approved by the MGH Radioactive Drug Research Committee.

Imaging session

Each subject underwent two MR–PET scans in a pseudo-randomized order, one as a baseline (not painful pressure) and the other with calibrated pressure pain applied. At least a 30 min-break was given for the subjects between the two scans. A serum pregnancy test (Sure-Vue serum hCG STAT) was performed on all female subjects prior to the scans to rule out current pregnancy. All images were acquired on a 3T Siemens TIM-Trio with a BrainPET insert (Siemens Healthcare, Erlangen, Germany). A PET-compatible CP transmit coil and an 8-channel receive array coil were used.

MRI

Gradient-echo EPI was used for BOLD imaging with the following parameters: TR/TE = 3000/30 ms, matrix = 72 × 72, field of view = 21.6 × 21.6 cm (3 mm isotropic resolution), and 47 slices without gaps. A dual-echo gradient-echo EPI with TR/TE1/TE2 = 4000/10/30 ms, labeling duration = 1.6 s, pot-labeling delay = 1 s, 3.4 × 3.4 × 6 mm spatial resolution, and GRAPPA (R = 2) acceleration, and 7/8 partial Fourier. A high-resolution T1-weighting anatomical image was acquired using multi-echo MPRAGE (TR = 2530 ms, TE1/TE2/TE3/TE4 = 1.64/3.5/5.36/7.22 ms, TI = 1200 ms, flip angle = 7°, and 1 mm isotropic). A dual ultra-short echo (DUTE) sequence with TR = 200 ms, TE1/TE2 = 0.07/2.24 ms, flip angle = 10°, and 1.67 mm isotropic resolution was run for deriving the PET attenuation map.

PET

Up to 12 mCi (10.77 ± 1.4 mCi, N = 16) of [^{11}C]diprenorphine, a non-selective opioid receptor antagonist, was injected intravenously as a manual bolus for each study. PET data were acquired for 90 min, stored in list mode format and binned into 44 frames of progressively longer duration (30 s × 10, 1 min × 15, 2 min × 15, 5 min × 4). The corresponding images were reconstructed using the 3D OP-OSEM algorithm with detector efficiency, decay, dead time, attenuation, and scatter corrections applied. The attenuation map was derived from the MPRAGE and DUTE data using an atlas-based classifier that allowed the segmentation of soft and bone tissue and air cavities (Poynton et al., 2012). The reconstructed volume consisted of 153 slices with

Please cite this article as: Wey, H.-Y., et al., Simultaneous fMRI–PET of the opioidergic pain system in human brain, NeuroImage (2014), http://dx.doi.org/10.1016/j.neuroimage.2014.07.058

256 × 256 pixels (1.25 × 1.25 × 1.25 mm^3). The spatial resolution at 8 cm radially from the center of the field of view was ~3 mm.

Pain stimulation

Calibrated pressure cuff pain was determined in the behavioral session and confirmed immediately before imaging. After the subject was positioned in the scanner, the pressure cuff was secured around subject's left calf muscle at the identical position as in the behavioral session. Two to four Low and High pain pressure stimuli, calibrated for each subject, were given to confirm the pressures selected produced the targeted rating.

The start of pressure pain was synchronized with radiotracer injection and the start of a BOLD fMRI scan. Intermittent calibrated pressure to achieve a High pain (15 out of 20 Gracely intensity scale) level was delivered for a total of 30 min (42 s ON with interstimulus OFF intervals of 4, 6 or 8 s). Subjects rated the pain intensity of each given stimulus using a button box during the interstimulus intervals. The pressure was adjusted in real-time to account for potential habituation. During baseline scans, stimuli at very low (30 mm Hg), non-painful, pressure were given to match the experimental conditions. No pain was experienced by the subjects as confirmed by subjective pain intensity rating as 0 for each given stimulus throughout the scan. Besides the given pressure, experimental paradigm and rating procedures were identical between the pain and non-painful pressure scans.

Data analysis

Data were processed using a combination of tools from FSL (FMRIB's Software Library, http://www.fmrib.ox.ac.uk/fsl) (Jenkinson et al., 2012), FreeSurfer (http://surfer.nmr.mgh.harvard.edu/fswiki), and PMOD (PMOD3.3, PMOD Technologies Ltd., Zurich, Switzerland) software packages.

MRI

BOLD fMRI data was first motion corrected (Jenkinson et al., 2002), skull stripped (Smith, 2002), and spatially smoothed with an 8 mm FHWM Gaussian kernel using FSL. Quality assurance procedures were carried out using Artifact Detection Tools (ART, http://www.nitrc.org/projects/artifact_detect) to identify outlier time points due to motion and/or signal spikes. Specifically, pre-processed fMRI data and the motion estimates obtained in the motion correction procedure (MCFLIRT in FSL) were imported into ART. An automatic process in ART was performed to calculate the global mean intensity. A time point in which signal intensity deviated more than 3 standard deviations of the global signal intensity or detected motion exceeded 0.5 mm from the previous time point was marked as an outlier. The outliers were exported and converted as confounds to be used later in first-level general linear model (GLM) analysis in FSL. A standard GLM analysis was used to generate the fMRI activation map. Individual subject's functional images were first registered to their own high-resolution anatomical images using boundary-based registration, and further registered to the standard MNI152 atlas space using affine linear registration with 12°-of-freedom (Greve and Fischl, 2009; Jenkinson and Smith, 2001). Statistical group analysis for different contrasts was performed using single-group average or two-group paired *t*-test in FSL ($Z > 2.3$ and cluster level $p < 0.05$ to account for multiple comparisons based on Gaussian Random Field theory). Significant clusters were converted from MNI to Talairach coordinates (Lancaster et al., 2007). Anatomical labels as well as the corresponding Brodmann areas were identified using the Talairach Daemon tool (Lancaster et al., 1997) and tabulated (Tables 1 and 2).

Individual subjects' high-resolution anatomical images were processed through the FreeSurfer reconstruction pipeline to generate subject specific, atlas-based regions of interests in order to extract time-activity curves (TACs) for PET kinetic modeling analysis (Fischl et al., 2004).

Table 1
Brain regions evoked by painful and non-painful pressure.

Regions	BA	Z_{max}	X	Y	Z	Cluster (voxels)
Pain						
R superior temporal/insula/postcentral gyrus (secondary sensory cortex)	13	4.52	−52	−6	6	4226
R caudate	NA	4.08	34	−42	4	2110
R inferior frontal gyrus	11	4.29	16	32	−18	2075
L middle temporal/insula	19/13	3.92	−54	−76	16	845
L postcentral gyrus (secondary sensory cortex)	6	4.11	−34	−20	32	677
L cerebellum	NA	4.49	−24	−88	−30	554
R anterior cingulate	32	2.57	20	32	8	41
R caudate	19	2.66	10	10	4	6
L superior temporal	47	2.44	−40	−36	14	6
Pressure (no pain)						
R superior temporal/insula	22	4.57	68	−20	4	4788
L transverse temporal gyrus	42	4.23	−64	−12	10	2684
R postcentral gyrus (primary sensory cortex)	2	4.12	40	−34	64	1696
L inferior frontal gyrus	47	4.06	−48	32	−18	1162
R anterior cingulate	25	3.61	4	18	−6	1023
L precuneus	31	3.41	−8	−48	30	567
R postcentral gyrus (primary sensory cortex)	3	2.81	56	−18	40	41
R inferior parietal lobule	40	2.94	72	−32	22	22
R postcentral gyrus	4	2.92	14	−34	58	20
R medial frontal gyrus	6	2.52	6	−26	70	4

PET

PET data was first motion corrected using rigid body linear registration (6° of freedom) to the middle time frame of the time series implemented in FSL (MCFLIRT) (Jenkinson et al., 2002). Kinetic modeling was carried out in PMOD using the subject-specific bilateral occipital cortices as the reference tissues. Quantitative binding potential maps (BP_{ND}), which represent the relative amount of specifically bound radioligand to that of non-displaceable radioligand, were calculated from the dynamic PET data on the basis of 0–60 min after radiotracer administration, similar to the previous studies (Sprenger et al., 2006; Zubieta et al., 2001). This time range was determined according to the dynamic of endogenous opioid release reported in a previous study (Scott et al., 2007) and similar to other studies (Sprenger et al., 2006; Zubieta et al., 2001). A modified simplified reference tissue model (SRTM2) was first used to estimate the individuals' k_2', the rate constant that describes the wash-out of the radioligand from the reference tissue, of

Table 2
Brain activations showed group differences between the painful and non-painful (pressure) conditions.

Regions	BA	Z_{max}	X	Y	Z	Cluster (voxels)
Pain > pressure						
L caudate	NA	4.46	−18	−18	30	5974
L thalamus	NA	4.1	−12	−4	8	
L putamen	NA	4.07	−22	−16	−2	
R thalamus	NA	4.06	8	−2	6	
R caudate	NA	4.04	16	−18	28	
R putamen	NA	4.02	24	−2	−4	
Brainstem (PAG)	NA	3.81	−4	−28	−8	1605
Brainstem						
L cerebellum	NA	3.75	−18	−80	−30	632
R inferior parietal gyrus	39/40	3.59	52	−66	44	414
R Supramarginal gyrus	40	3.18	62	−54	38	
Pressure > pain						
R precuneus	31	3.59	4	−74	34	1629
R posterior cingulate	30	3.41	22	−54	14	
L medial frontal gyrus	6	3.64	0	−2	58	1248
L paracentral gyrus	4/5	3.61	−4	−32	60	
R medial frontal gyrus	6	3.53	10	−2	54	
L cingulate gyrus	24	3.53	−6	4	48	
L cuneus	18	3.61	−4	−96	16	427

Please cite this article as: Wey, H.-Y., et al., Simultaneous fMRI–PET of the opioidergic pain system in human brain, NeuroImage (2014), http://dx.doi.org/10.1016/j.neuroimage.2014.07.058

a high-binding region (i.e. thalamus) (Wu and Carson, 2002), and this value was subsequently applied in the kinetic modeling with the non-invasive Logan model (Logan et al., 1996). The time until linearity of the Logan plot achieved was determined for each scan ($t = 7.5 \pm 2.9$ min for baseline scans and $t = 8.4 \pm 3.8$ min for pain scans, $p > 0.5$). The resulting BP_{ND} images were co-registered to the MNI152 space for group analysis. The co-registration of PET data was achieved using transformation matrixes derived from the simultaneously acquired anatomical MRI images to minimize the potential variability of registering low resolution PET data to the MNI atlas brain. Group averaged BP_{ND} maps for the nonpainful and pain scans as well as the difference maps (nonpainful–pain) were calculated (Fig. 2). Statistical group analysis was performed using a two-group paired *t*-test. In accordance with the previous studies (Bencherif et al., 2002; Sprenger et al., 2006; Zubieta et al., 2001), we defined a priori brain regions of relevance for pain perception and modulation, including bilateral anterior and posterior insula, amygdala, hippocampus, hypothalamus, striatum (includes caudate, putamen, global pallidus, and nucleus accumbens), thalamus, orbitofrontal cortex (includes frontal medial cortex and subcallosal cortex), and bilateral superior temporal cortices to correct for multiple comparisons with a cluster-based correction at $p < 0.05$ and a cluster-forming $Z > 2.3$. All of the above mentioned structures were identified and selected based on the Harvard–Oxford cortical and subcortical atlases, with the exception of the hypothalamus. Bilateral hypothalamus was identified using the Wake Forest University Pick Atlas (http://fmri.wfubmc.edu/software/PickAtlas). Significant clusters were identified and tabulated (Fig. 3a and Table 3). In addition, regional BP_{ND} values of the thalamus, the pumatem/NAc and the OFC regions were extracted from both scans from each subject, and plotted in Fig. 3b to show inter-subject variability.

Correlation analysis

To investigate the relationships between fMRI and PET signal changes, ROIs were chosen a posterior from the only two overlapping fMRI–PET activations in the right ventral striatum (putamen/NAc) and the left thalamus (Fig. 4). The ROIs were then applied to both PET and BOLD fMRI images to extract BP_{ND} and percent BOLD signal change (using FSL featquery) from each individual subject. Spearman correlation analysis was done to assess correlations between PET BP_{ND} and fMRI %BOLD signal changes (pain > non-painful pressure) (Fig. 5) using GraphPad Prism 5 (GraphPad Software, Inc., La Jolla, USA).

Results

The pressure delivered to induce deep tissue pain on the left calf muscle was 310 ± 90 mm Hg (mean ± SD) for our cohort, which resulted in a mean intensity pain rating of 13 ± 2 (mean ± SD) using the 0–20 Gracely scale (Gracely et al., 1978). During the control scans, a pressure of only 30 mm Hg was delivered following the same paradigm; all subjects reported pain intensity as 0 (no pain) throughout the scan.

FMRI data analysis reveals typical robust responses to both pain and nonpainful pressure stimulation (Fig. 1 and Table 1). The result showed that during pressure pain stimulation, significant BOLD fMRI activations were observed in secondary sensory cortices, insula, anterior cingulate, striatum, inferior fontal regions and cerebellum. Direct comparison between the pain and nonpainful pressure conditions shows that painful pressure evokes significantly greater fMRI signal changes in bilateral thalamus, caudate, putamen, periaqueductal gray (PAG), rostral ventromedial medulla (RVM), and cerebellum (Fig. 1b and Table 2); while nonpainful pressure evokes more fMRI signal changes in supplementary motor area, posterior cingulate, and precuneus/cuneus (Table 2). The PAG and RVM are part of the descending pain modulatory network (Kong et al., 2010b). However, it is possible that a brain region being identified when comparing nonpainful pressure > pain could indeed show a less negative change during nonpainful than painful pressure. Future studies utilize quantitative MRI technique (such as arterial spin labeling) could potentially help clarify this confound.

PET TACs demonstrate a typical wash-in and slow washout characteristic following bolus injections of [^{11}C]DPN similar to what has been shown previously (Maarrawi et al., 2007). Group averaged BP_{ND} maps showed higher BP_{ND} values in bilateral thalamus, striatum, insula, orbitofrontal cortex, and cingulate cortices in the nonpainful pressure scan than those obtained from the pressure pain condition (Fig. 2). Voxel-wise statistical comparison of [^{11}C]DPN BP_{ND} as measured by PET revealed pain-associated decreases in contralateral (right) posterior insula, contralateral amygdala, orbitofrontal cortex, and bilaterally in thalamus, caudate, putamen, nucleus accumbens (NAc), hippocampus/parahippocampus, and superior temporal gyrus (Fig. 3a and Table 3). These data suggest that the presence of sustained pain causes regionally specific release of endogenous opioids resulting in competition with either the radiotracer for binding sites or rapid receptor internalization. Individual changes of in vivo opioid receptor availability during painful and non-painful pressure are presented in Fig. 3b. The results show across subjects a high consistency in the downward direction of change between BP_{ND} during non-painful and painful states. The average percent reduction in BP_{ND} is 11% in the contralateral ventral striatum (putamen/NAc), 24% in the orbitofrontal region, and 16% in the ipsilateral thalamus.

In addition to distinct brain networks as measured by PET and fMRI, we also found fMRI signal increases and BP_{ND} decreases (pain > non-painful pressure) overlapped in regions of the ipsilateral thalamus and contralateral ventral striatum (putamen/NAc) (Fig. 4). To examine the relationship between fMRI and PET changes in these overlapping regions, we performed a Spearman correlation analysis on the stimulus-evoked fMRI and PET signal changes across subjects. Note that BP_{ND} decreases were used to compare with BOLD fMRI signal increase (pain > non-painful pressure) since the degree of BP_{ND} reduction correlates with the amount of endogenous neurotransmitter release (Endres et al., 1997; Laruelle, 2000). We found a significant positive correlation between PET BP_{ND} changes (nonpainful pressure–pain) and BOLD percent signal changes (pain–nonpainful pressure) in the ipsilateral thalamus (Spearman $r = 0.98$, $p = 0.0004$). Fig. 5 suggests a coherent response between the BOLD signal change and the underlying opioid receptor activation in the thalamus. No correlation between PET BP_{ND} and fMRI signal change was found in the only other area of overlap, the contralateral ventral striatum (putamen/NAc) (Fig. 5; Spearman $r = -0.33$, $p = 0.43$).

Table 3
Brain regions show BP_{ND} changes as measured by PET ($P_{corr} < 0.05$).

Regions	BA	Z_{max}	X	Y	Z	Cluster (voxels)
R orbitofrontal area (rectal gyrus)	11	3.25	2	36	−28	336
R middle temporal gyrus	22	3.28	54	−34	0	162
L hippocampus	NA	2.96	−30	−38	−8	115
R superior temporal gyrus	22	3.09	56	−8	−14	114
R amygdala	NA	2.86	24	0	−18	99
R putamen	NA	2.84	28	4	−4	96
R thalamus	NA	3.01	12	−32	2	77
R parahippocampal gyrus	28	3.04	22	−14	−16	62
L thalamus	NA	2.83	−10	−14	0	54
R putamen (medial GP)	NA	2.98	22	−12	−2	42
L caudate (caudate head)	NA	2.66	−8	12	−10	34
R claustrum	NA	3	38	−18	−2	33
L putamen (lateral GP)	NA	2.68	−26	−16	4	33
R insula	13	2.73	42	−8	8	28
R hypothalamus	NA	2.67	8	−2	−10	19

Discussion

In the present study, we report the first simultaneous fMRI–PET pain imaging in humans. We investigate changes of BOLD fMRI and PET

Please cite this article as: Wey, H.-Y., et al., Simultaneous fMRI–PET of the opioidergic pain system in human brain, NeuroImage (2014), http://dx.doi.org/10.1016/j.neuroimage.2014.07.058

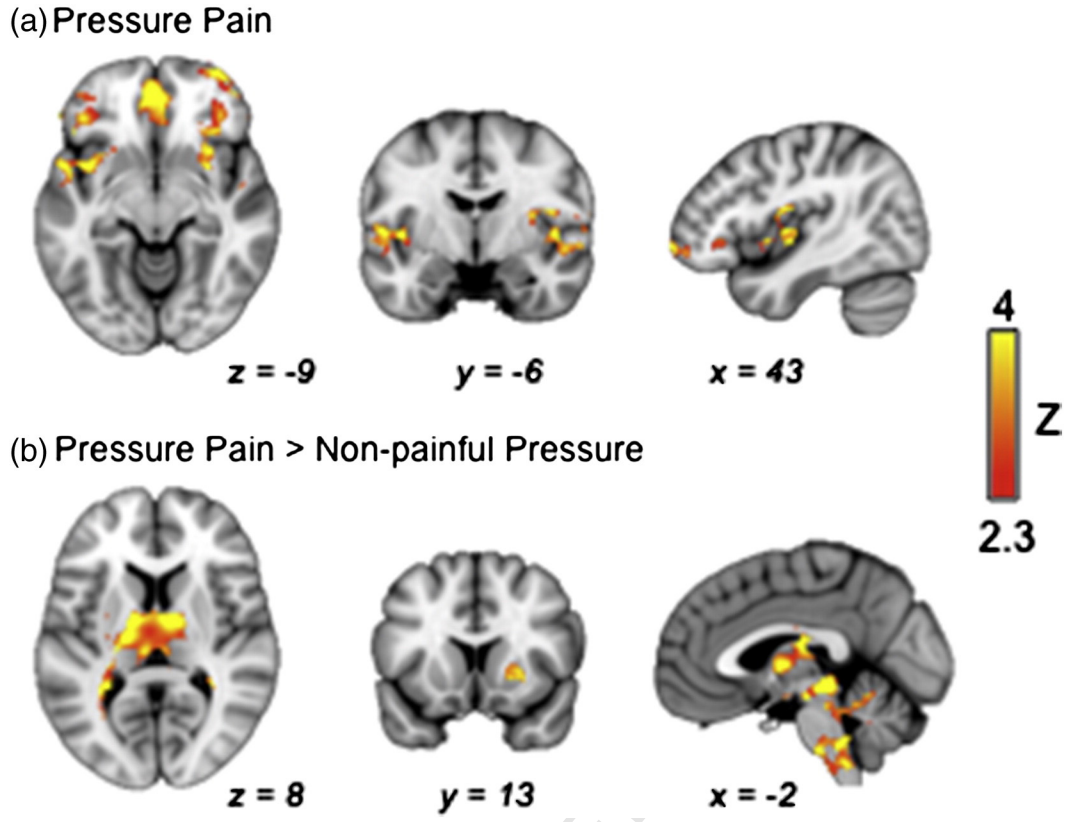

Fig. 1. BOLD-fMRI activation maps in responses to external pain stimuli in a group of healthy volunteers. Brain regions involved in (a) pressure pain processes and (b) pressure pain > non-painful pressure as measured by BOLD fMRI from simultaneous PET/MRI scans.

receptor binding potential of an opioid ligand, [^{11}C]DPN, in response to experimental pressure pain. The results of our study reveal co-localized fMRI and [^{11}C]DPN PET activations in the thalamus and striatum in addition to distinct modality-specific brain regions related to pain processing. By examining the concurrent fMRI and PET responses during pain experience, our results suggest a distinct role of endogenous opioid neurotransmission on hemodynamic responses in different brain regions.

Our fMRI results are consistent with the previous findings that report the involvement of secondary sensory cortices, prefrontal cortex, insula, thalamus, basal ganglia, and ACC (Kong et al., 2010a; Tracey and Mantyh, 2007). These regions are of relevance for sensory processing/discrimination, as well as the affective aspect of sensory stimulation (Tracey and Mantyh, 2007). We did not find activation in the primary sensory cortex. The discrepancy between our results and the literature might be related to different experimental pain used.

Our PET results are also consistent with the previous pain imaging studies, in which decreases in receptor availability (as measured by [^{11}C]carfentanil BP_{ND}) were seen in the bilateral thalamus, ipsilateral amygdala, hypothalamus, and insula (Bencherif et al., 2002; Scott et al., 2007; Zubieta et al., 2001). Although Bencherif et al. reported changes in receptor BP_{ND} in the contralateral thalamus, the other two studies showed decreases in receptor availability bilaterally. It has been suggested that brain activations related to peripheral pain may be symmetrical as oppose to an asymmetric pattern associated with central pain (Kong et al., 2010a; Maarrawi et al., 2007). Although we did observe bilateral reduction in [^{11}C]DPN BP_{ND} (Fig. 2), the magnitude of BP_{ND} reduction is larger on the ipsilateral side than the contralateral side. This discrepancy could potentially due to 1) the involvement of pathological conditions (Maarrawi et al., 2007); 2) the type of stimulation being applied (Kong et al., 2010a); and/or 3) our relatively small sample size. In addition, we found the involvement of orbitofrontal cortex, and caudate, putamen, NAc, and hippocampus/parahippocampus bilaterally. We speculate the densities of δ- and κ- opioid receptors. Q4 Consistent with the [^{11}C]carfentanil studies, no region displayed increased BP_{ND} in response to pain (Sprenger et al., 2006; Zubieta et al., 2001). The percent changes calculated in the present study are on the order of 10–25%, which are comparable to those reported with other experimental pain paradigms using the specific μ-opioid receptor agonist, [^{11}C]carfentanil (Zubieta et al., 2001). It is also worth noting that the percent BP_{ND} changes detected here are induced by a physiological challenge, and the magnitude of changes is of the same order as those observed during pharmacological challenges known to cause large changes in receptor occupancy (~50% with intravenously injected opioid antagonist—naloxone) (Jones et al., 1994; Melichar et al., 2003). This result underscores the power of the endogenous opioid system to self-regulate in response to external stimuli.

We found a significantly positive correlation between BOLD and BP_{ND} signal changes in the thalamus. The fMRI–PET activations overlapping in the medial thalamic sub-region, which have been reported previously for pain induced opioid release (Scott et al., 2007). The thalamus is important for sensory discrimination, transmission/modulation of painful stimuli, and is also a key structure associated with chronic pain development (Tracey and Bushnell, 2009) and pathology of different chronic pain conditions (Martikainen et al., 2013). An earlier study showed that opioid receptor activation (as measured by changes in BP_{ND}) in the thalamus is associated with sensory and affective response attenuation to sustained pain (Zubieta et al., 2001). Our results are consistent with the interpretation that noxious pressure induces endogenous opioids release in the thalamus, and endogenous opioids cause a general inhibition in the thalamic neurons (Henriksen and Willoch, 2008). Thus, our results provide direct evidence of thalamic contribution to opioid related pain-modulation. A reduction in excitatory neurotransmitter release, such as glutamate, is also possible in response to opioid release (Henriksen and Willoch, 2008), but it does not account for the increase in fMRI signal. Our study design, enabled by

Please cite this article as: Wey, H.-Y., et al., Simultaneous fMRI–PET of the opioidergic pain system in human brain, NeuroImage (2014), http://dx.doi.org/10.1016/j.neuroimage.2014.07.058

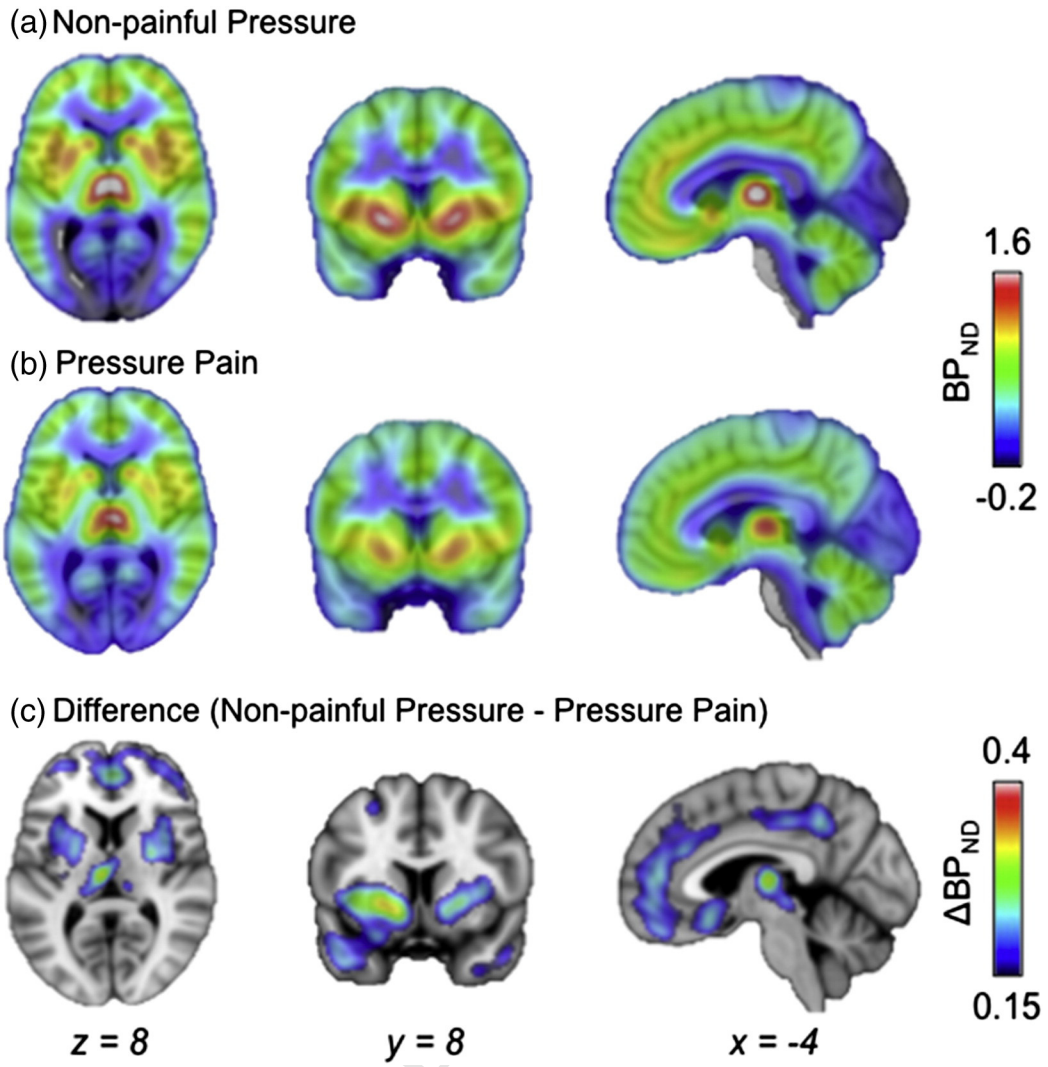

Fig. 2. Averaged binding potential (BP_{ND}) maps from the (a) nonpainful and (b) painful pressure scans as well as the (c) BP_{ND} difference maps. A reduction in BP_{ND} was shown in the thalamus, striatum, cingulate cortices, and orbitofrontal regions.

simultaneous fMRI–PET, provides a more direct method to assess the neurochemical underpinnings of BOLD signal than using each imaging modality alone. Exploring fMRI and PET signal correlations provides potentially useful information to facilitate our understanding of how hemodynamic responses change with brain neurochemistry. However, it should be noted that due to our relatively small sample size, interpretations of the correlation analysis results should be considered with caution.

No correlation between BOLD and BP_{ND} signal changes was observed in the striatum (putamen/NAc). There are several reasons that could account for this finding. The simplest explanation is that there are more neurochemical sources for the BOLD signal in this region. For example, ventral striatum is known for its role in reward processing and is densely innervated by dopaminergic afferents. Accumulating evidence indicates extensive shared anatomical substrates of painful and pleasant sensations (Leknes and Tracey, 2008). It has also been shown that opioids modulate dopaminergic neurotransmission in the mesolimbic pathway through dis-inhibiting GABAergic interneurons (Hagelberg et al., 2002; Shih et al., 2012). Animal studies have reported dopamine release in NAc in response to prolonged, but not brief, pain stimulation (Louilot et al., 1986; Schmidt et al., 2002). BOLD signal changes thus likely reflect the contributions of not only the opioid mediated dis-inhibition of the GABAergic projection neurons, but also the increased activity of the dopaminergic neurons. Another potential explanation for the differences between the thalamic and putamen/NAc responses is the differential cerebral vascular effects of endogenous opioids in these two brain regions. In response to opioid agonists, cerebral blood flow decreases in striatum and thalamus, midbrain structures were reported while cerebral blood flow increases in medial prefrontal/frontal, parietal and occipital cortices were shown in both human and animal studies (Liu et al., 2007; Wagner et al., 2007). Potential Q5 co-activation of the opioid and dopamine systems might have different influences on neurovascular coupling and vascular tone. Nevertheless, due to the small sample size of the current study, future studies are needed in order to better understand the impact of neurotransmission on neurovascular coupling in human subjects.

Conclusions

In summary, we demonstrate the feasibility of concurrently measuring endogenous opioid release and BOLD responses during experimental pain using simultaneous fMRI–PET. The distinct but overlapping networks, each revealing different aspects of cerebral pain processing, highlight the value of this new technology to contribute to our understanding of brain function. The majority of the brain regions within the extensive network of pain-related BOLD activations did not co-localize with any changes in opioid receptor binding suggesting that these are not likely sites for direct opioid mediated pain modulation.

Please cite this article as: Wey, H.-Y., et al., Simultaneous fMRI–PET of the opioidergic pain system in human brain, NeuroImage (2014), http://dx.doi.org/10.1016/j.neuroimage.2014.07.058

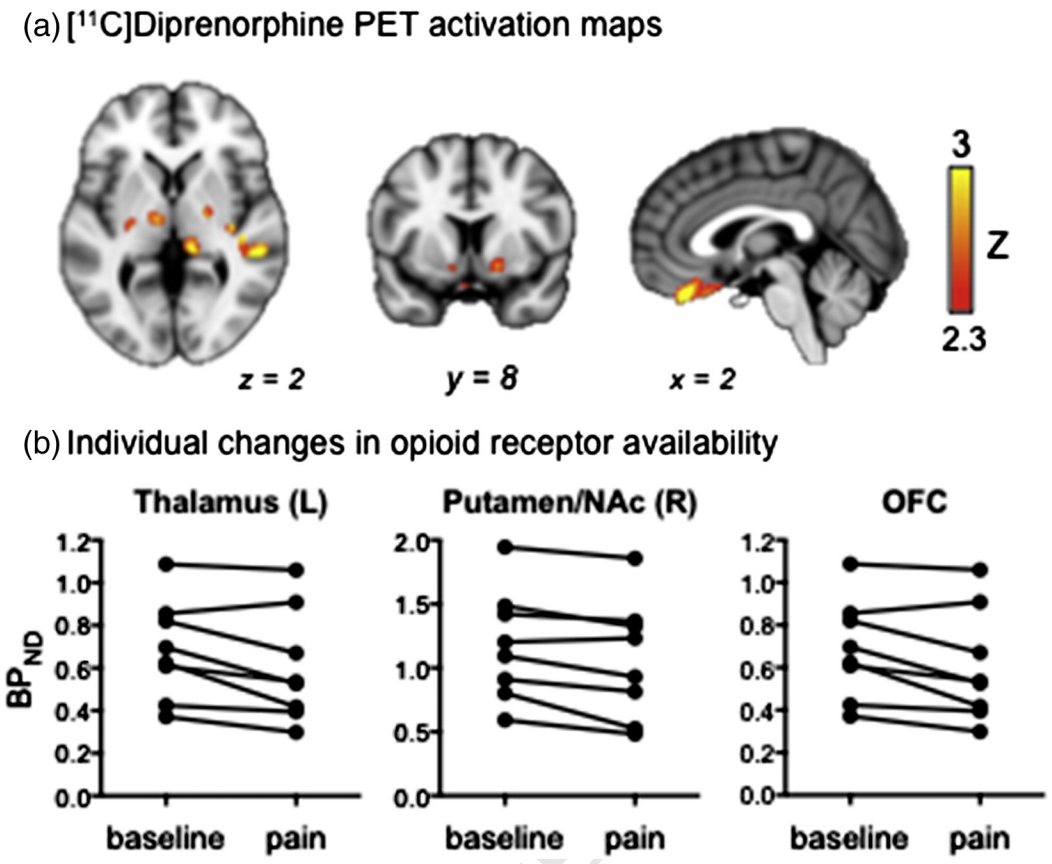

Fig. 3. Brain activation detected by [^{11}C]diprenorphine PET in responses to external pain stimuli in a group of healthy volunteers. (a) PET detected binding potential (BP_{ND}) changes between nonpainful pressure and pain conditions. Signal changes indicate decreases in receptor availability during pain, which indicates endogenous opioid releases. (b) Individual changes in opioid receptor availability are shown for ipsilateral (left) thalamus (Thalamus (L)), contralateral (right) ventral striatum (putamen/nucleus accumbens) (Putamen/NAc (R)), and orbitofrontal cortex (OFC).

Future studies empowered with a larger sample size are needed to confirm this conclusion and to explore the possible neuroreceptor-based functional networks. The positive correlation of the co-localized BOLD activation and PET BP_{ND} change in the thalamus suggest that the consequence of pain-induced changes in endogenous opioid neurotransmission is a major source of the BOLD signal in this region. The uncorrelated co-localized BOLD activation and PET BP_{ND} change in the striatum (putamen/NAc) suggest that multiple additional receptor systems contribute to the BOLD signal in this region. Future fMRI–PET studies collecting dynamic quantitative regional hemodynamics (such as cerebral blood flow or cerebral blood volume) with other receptor ligands (such as dopamine receptor selective radiotracers) will further characterize the effects of specific neuroreceptor systems on pain induced BOLD activation. Simultaneous fMRI–PET offers a valuable new approach allowing us to disentangle specific neurochemical contributions to the composite BOLD signal, as well as other hemodynamic fMRI responses and neurovascular coupling, with exquisite spatial and temporal resolution.

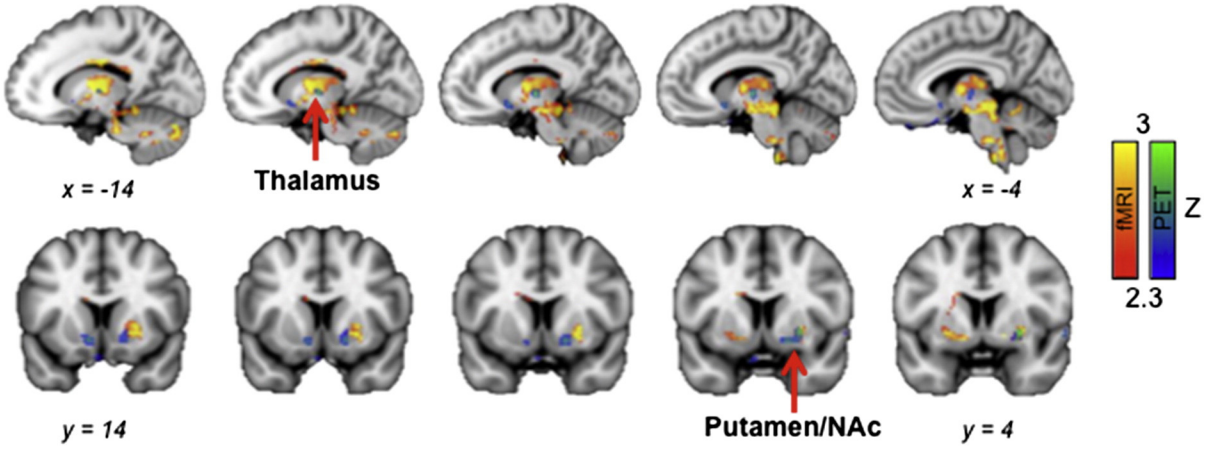

Fig. 4. fMRI–PET activation overlaps in responses to external pain stimuli in a group of healthy volunteers. Spatial overlap of receptor activation as measured as decreases in BP_{ND} (PET, blue–green) and BOLD fMRI (pain > non-painful pressure, red–yellow) was shown in the thalamus and striatum (putamen/nucleus accumbens) (Putamen/NAc).

Please cite this article as: Wey, H.-Y., et al., Simultaneous fMRI–PET of the opioidergic pain system in human brain, NeuroImage (2014), http://dx.doi.org/10.1016/j.neuroimage.2014.07.058

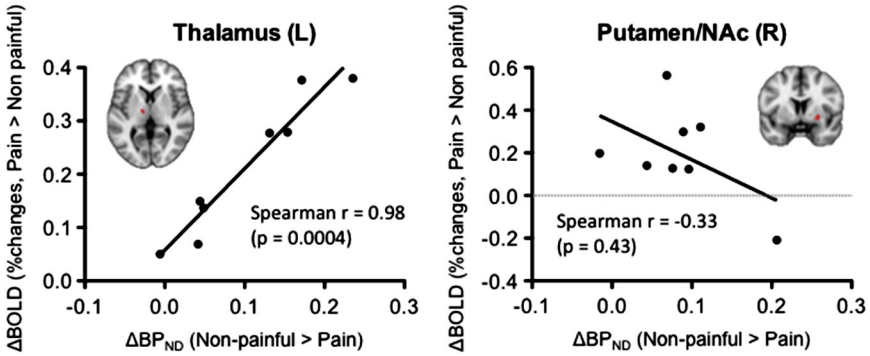

Fig. 5. Correlation analysis of fMRI–PET signal changes in brain regions showed activation overlaps. Scatter plots between fMRI and PET signal changes in the overlapped brain regions. Spearman correlation analysis showed a significantly positive correlation in ipsilateral thalamus (Spearman $r = 0.98$, $p < 0.005$) and no correlation in the contralateral ventral striatum (putamen/nucleus accumbens) (Putamen/NAc (R)). Brain inlets show the brain regions with activation overlaps.

Acknowledgments

The authors thank Patricia McCarthy, NP for her help on placing i.v. lines and monitoring subject condition during scans; Grae Arabasz and Shirley Hsu for their assistance with radiotracer administration; and Steve Carlin and Chris Moseley for radiotracer synthesis. We also thank Ms. Amanda Cook, Xiaoyan Chen, Rosa Spaeth, and Lisette Roman for the subject recruitment and assistance with the experiments. This work was supported by R03-AT218317 (NIDA), R01-AT006364 (NIH/NCCAM) to Jian Kong, R01-AT005280 (NIH/NCCAM) to Randy Gollub, and P01-AT006663-01 (NIH/NCCAM) to Bruce Rosen.

Competing financial interests

The authors declare no competing financial interests.

References

Bencherif, B., Fuchs, P.N., Sheth, R., Dannals, R.F., Campbell, J.N., Frost, J.J., 2002. Pain activation of human supraspinal opioid pathways as demonstrated by [^{11}C]-carfentanil and positron emission tomography (PET). Pain 99, 589–598.

Catana, C., Drzezga, A., Heiss, W.-D., Rosen, B.R., 2012. PET/MRI for neurologic applications. J. Nucl. Med. 53, 1916–1925.

Catana, C., Wu, Y., Judenhofer, M.S., Qi, J., Pichler, B.J., Cherry, S.R., 2006. Simultaneous acquisition of multislice PET and MR images: initial results with a MR-compatible PET scanner. J. Nucl. Med. 47, 1968–1976.

Drzezga, A., Souvatzoglou, M., Eiber, M., Beer, A.J., Furst, S., Martinez-Möller, A., Nekolla, S.G., Ziegler, S., Ganter, C., Rummeny, E.J., Schwaiger, M., 2012. First clinical experience with integrated whole-body PET/MR: comparison to PET/CT in patients with oncologic diagnoses. J. Nucl. Med. 53, 845–855.

Endres, C.J., Kolachana, B.S., Saunders, R.C., Su, T., Weinberger, D., Breier, A., Eckelman, W.C., Carson, R.E., 1997. Kinetic modeling of [^{11}C]raclopride: combined PET-microdialysis studies. J. Cereb. Blood Flow Metab. 17, 932–942.

Falkenberg, L.E., Westerhausen, R., Specht, K., Hugdahl, K., 2012. Resting-state glutamate level in the anterior cingulate predicts blood–oxygen level-dependent response to cognitive control. Proc. Natl. Acad. Sci. U. S. A. 109, 5069–5073.

Fischl, B., van der Kouwe, A., Destrieux, C., Halgren, E., Ségonne, F., Salat, D.H., Busa, E., Seidman, L.J., Goldstein, J., Kennedy, D., Caviness, V., Makris, N., Rosen, B., Dale, A.M., 2004. Automatically parcellating the human cerebral cortex. Cereb. Cortex 14, 11–22.

Gracely, R., McGrath, P., Dubner, R., 1978. Validity and sensitivity of ratio scales of sensory and affective verbal pain descriptors: manipulation of affect by diazepam. Pain 5, 19–29.

Greve, D.N., Fischl, B., 2009. Accurate and robust brain image alignment using boundary-based registration. NeuroImage 48, 63–72.

Hagelberg, N., Kajander, J.K., Någren, K., Hinkka, S., Hietala, J., Scheinin, H., 2002. Mu-receptor agonism with alfentanil increases striatal dopamine D2 receptor binding in man. Synapse 45, 25–30.

Henriksen, G., Willoch, F., 2008. Imaging of opioid receptors in the central nervous system. Brain 131, 1171–1196.

Jenkins, B.G., 2012. Pharmacologic magnetic resonance imaging (phMRI): imaging drug action in the brain. NeuroImage 62, 1072–1085.

Jenkinson, M., Bannister, P., Brady, M., Smith, S., 2002. Improved optimization for the robust and accurate linear registration and motion correction of brain images. NeuroImage 17, 825–841.

Jenkinson, M., Beckmann, C.F., Behrens, T.E.J., Woolrich, M.W., Smith, S.M., 2012. FSL. NeuroImage 62, 782–790.

Jenkinson, M., Smith, S., 2001. A global optimisation method for robust affine registration of brain images. Med. Image Anal. 5, 143–156.

Jones, A.K., Cunningham, V.J., Ha-Kawa, S.K., Fujiwara, T., Liyii, Q., Luthra, S.K., Ashburner, J., Osman, S., Jones, T., 1994. Quantitation of [11C]diprenorphine cerebral kinetics in man acquired by PET using presaturation, pulse-chase and tracer-only protocols. J. Neurosci. Methods 51, 123–134.

Kong, J., Gollub, R.L., Polich, G., Kirsch, I., LaViolette, P., Vangel, M., Rosen, B., Kaptchuk, T.J., 2008. A functional magnetic resonance imaging study on the neural mechanisms of hyperalgesic nocebo effect. J. Neurosci. 28, 13354–13362.

Kong, J., Gollub, R.L., Rosman, I.S., Webb, J.M., Vangel, M.G., Kirsch, I., Kaptchuk, T.J., 2006a. Brain activity associated with expectancy-enhanced placebo analgesia as measured by functional magnetic resonance imaging. J. Neurosci. 26, 381–388.

Kong, J., Loggia, M.L., Zyloney, C., Tu, P., LaViolette, P., Gollub, R.L., 2010a. Exploring the brain in pain: activations, deactivations and their relation. Pain 148, 257–267.

Kong, J., Tu, P.-c, Zyloney, C., Su, T.-p, 2010b. Intrinsic functional connectivity of the periaqueductal gray, a resting fMRI study. Behav. Brain Res. 211, 215–219.

Kong, J., White, N.S., Kwong, K.K., Vangel, M.G., Rosman, I.S., Gracely, R.H., Gollub, R.L., 2006b. Using fMRI to dissociate sensory encoding from cognitive evaluation of heat pain intensity. Hum. Brain Mapp. 27, 715–721.

Lancaster, J.L., Rainey, L.H., Summerlin, J.L., Freitas, C.S., Fox, P.T., Evans, A.C., Toga, A.W., Mazziotta, J.C., 1997. Automated labeling of the human brain: a preliminary report on the development and evaluation of a forward-transform method. Hum. Brain Mapp. 5, 238–242.

Lancaster, J.L., Tordesillas-Gutiérrez, D., Martinez, M., Salinas, F., Evans, A., Zilles, K., Mazziotta, J.C., Fox, P.T., 2007. Bias between MNI and Talairach coordinates analyzed using the ICBM-152 brain template. Hum. Brain Mapp. 28, 1194–1205.

Laruelle, M., 2000. Imaging synaptic neurotransmission with in vivo binding competition techniques: a critical review. J. Cereb. Blood Flow Metab. 20, 423–451.

Leknes, S., Tracey, I., 2008. A common neurobiology for pain and pleasure. Nat. Rev. Neurosci. 9, 314–320.

Liu, C.H., Greve, D.N., Dai, G., Marota, J.J.A., Mandeville, J.B., 2007. Remifentanil administration reveals biphasic phMRI temporal responses in rat consistent with dynamic receptor regulation. NeuroImage 34, 1042–1053.

Logan, J., Fowler, J.S., Volkow, N.D., Wang, G.J., Ding, Y.S., Alexoff, D.L., 1996. Distribution volume ratios without blood sampling from graphical analysis of PET data. J. Cereb. Blood Flow Metab. 16, 834–840.

Louilot, A., Le Moal, M., Simon, H., 1986. Differential reactivity of dopaminergic neurons in the nucleus accumbens in response to different behavioral situations. An in vivo voltammetric study in free moving rats. Brain Res. 397, 395–400.

Maarrawi, J., Peyron, R., Mertens, P., Costes, N., Magnin, M., Sindou, M., Laurent, B., Garcia-Larrea, L., 2007. Differential brain opioid receptor availability in central and peripheral neuropathic pain. Pain 127, 183–194.

Martikainen, I.K., Peciña, M., Love, T.M., Nuechterlein, E.B., Cummiford, C.M., Green, C.R., Harris, R.E., Stohler, C.S., Zubieta, J.-K., 2013. Alterations in endogenous opioid functional measures in chronic back pain. J. Neurosci. 33, 14729–14737.

Melichar, J.K., Nutt, D.J., Malizia, A.L., 2003. Naloxone displacement at opioid receptor sites measured in vivo in the human brain. Eur. J. Pharmacol. 459, 217–219.

Muthukumaraswamy, S.D., Evans, C.J., Edden, R.A.E., Wise, R.G., Singh, K.D., 2012. Individual variability in the shape and amplitude of the BOLD-HRF correlates with endogenous GABAergic inhibition. Hum. Brain Mapp. 33, 455–465.

Northoff, G., Walter, M., Schulte, R.F., Beck, J., Dydak, U., Henning, A., Boeker, H., Grimm, S., Boesiger, P., 2007. GABA concentrations in the human anterior cingulate cortex predict negative BOLD responses in fMRI. Nat. Neurosci. 10, 1515–1517.

Poynton, C., Chonde, D., Sabunca, M., Kong, J., Gollub, R.L., Hooker, J.M., Catana, C., 2012. Atlas-based segmentation of T1-weighted and Dute MRI for calculation of attenuation correction maps in PET-MRI of brain tumor patients. J. Nucl. Med. 2332.

Schmidt, B.L., Tambeli, C.H., Barletta, J., Luo, L., Green, P., Levine, J.D., Gear, R.W., 2002. Altered nucleus accumbens circuitry mediates pain-induced antinociception in morphine-tolerant rats. J. Neurosci. 22, 6773–6780.

Scott, D.J., Stohler, C.S., Koeppe, R.A., Zubieta, J.-K., 2007. Time-course of change in [^{11}C] carfentanil and [^{11}C]raclopride binding potential after a nonpharmacological challenge. Synapse 61, 707–714.

Shih, Y.-Y.I., Chiang, Y.-C., Shyu, B.-C., Jaw, F.-S., Duong, T.Q., Chang, C., 2012. Endogenous opioid–dopamine neurotransmission underlie negative CBV fMRI signals. Exp. Neurol. 234, 382–388.
Smith, S.M., 2002. Fast robust automated brain extraction. Hum. Brain Mapp. 17, 143–155.
Sprenger, T., Valet, M., Boecker, H., Henriksen, G., Spilker, M.E., Willoch, F., Wagner, K.J., Wester, H.J., Tölle, T.R., 2006. Opioidergic activation in the medial pain system after heat pain. Pain 122, 63–67.
Tracey, I., Bushnell, M.C., 2009. How neuroimaging studies have challenged us to rethink: is chronic pain a disease? J. Pain 10, 1113–1120.
Tracey, I., Mantyh, P.W., 2007. The cerebral signature for pain perception and its modulation. Neuron 55, 377–391.
Wagner, K.J., Sprenger, T., Kochs, E.F., Tölle, T.R., Valet, M., Willoch, F., 2007. Imaging human cerebral pain modulation by dose-dependent opioid analgesia: a positron emission tomography activation study using remifentanil. Anesthesiology 106, 548–556.
Willoch, F., Tölle, T.R., Wester, H.J., Munz, F., Petzold, A., Schwaiger, M., Conrad, B., Bartenstein, P., 1999. Central pain after pontine infarction is associated with changes in opioid receptor binding: a PET study with 11C-diprenorphine. AJNR Am. J. Neuroradiol. 20, 686–690.
Wu, Y., Carson, R.E., 2002. Noise reduction in the simplified reference tissue model for neuroreceptor functional imaging. J. Cereb. Blood Flow Metab. 22, 1440–1452.
Zubieta, J.K., Smith, Y.R., Bueller, J.A., Xu, Y., Kilbourn, M.R., Jewett, D.M., Meyer, C.R., Koeppe, R.A., Stohler, C.S., 2001. Regional mu opioid receptor regulation of sensory and affective dimensions of pain. Science 293, 311–315.

Please cite this article as: Wey, H.-Y., et al., Simultaneous fMRI–PET of the opioidergic pain system in human brain, NeuroImage (2014), http://dx.doi.org/10.1016/j.neuroimage.2014.07.058